Experimental reservoir computing using VCSEL polarization dynamics

Jeremy Vatin, Damien Rontani, Marc Sciamanna

Research Article | Vol. 27, No. 13 | 24 Jun 2019 | OPTICS EXPRESS 18579
Optics EXPRESS

Experimental reservoir computing using VCSEL polarization dynamics

JEREMY VATIN,[1,2,*] DAMIEN RONTANI,[1,2] AND MARC SCIAMANNA[1,2]

[1] *Chaire Photonique, CentraleSupélec and Université Paris-Saclay, 2 rue Edouard Belin, Metz F-57070, France*
[2] *Université de Lorraine and CentraleSupélec, LMOPS, 2 rue Edouard Belin, Metz F-57000, France*
[*] *jeremy.vatin@centralesupelec.fr*

Abstract: We realize an experimental setup of a time-delay reservoir using a VCSEL with optical feedback and optical injection. The VCSEL is operated in the injection-locking regime. This allows us to solve different information processing tasks, such as chaotic time-series prediction with a NMSE of 1.6×10^{-2} and nonlinear channel equalization with a SER of 1.5×10^{-2}, improving state-of-the-art performance. We also demonstrate experimentally, through a careful statistical analysis, the impact of the VCSEL polarization dynamics on the performance of our architecture. More specifically, we confirm recent theoretical prediction stating that a polarization rotated feedback allows for the enhancement of the calculation performance compared to an isotropic feedback.

The need for efficient data processing has led to the development of novel computing methods to solve tasks that conventional computers would struggle with [1, 2] : For example, pattern recognition, automatic signal classification, or time-series prediction. Among these methods, the reservoir computing approach, developed within the framework of Machine Learning, allows using photonic systems to form an artificial neural network with a simplified training procedure : only the readout layer is trained with a linear regression [3]. Multiple experimental implementations of reservoir computers have already been proposed and demonstrated good computing ability [4–6].

Because of the technical challenge consisting of interconnecting a large number of photonic units together, another architecture was proposed : the time-delay reservoir [7]. This approach allows using a single photonic node in combination with a large number of virtual nodes spread over different locations in the time-delay line. As a result, the number of nodes in the architecture can be simply increased by changing the length of a delay line. Several implementations have been proposed : the optoelectronic [8, 9] or all-optical configurations [10–13].

The efficiency of these systems strongly depends on the tuning of the different physical parameters, and on the complexity of the dynamics of the nonlinear node. That is why adding other degrees of freedom can help improving their performance. For example, Hicke *et al.* in [14] added the control of the polarization of an edge-emitting laser along a feedback loop, and concluded theoretically that using the specific configuration of polarization rotated feedback improves the performance of their system in some ranges of operational parameters. We extend this work in several ways, replacing this conventional edge-emitting laser diode by a vertical-cavity laser diode (VCSEL). It eases the possibility to tune the polarization properties of the physical node. This VCSEL-based reservoir computer seems particularly adapted to perform calculation. It exhibits interesting polarization dynamics that allows generating much coupled information in a same period of time and thus improves the computing ability and the memory capacity of the reservoir, as we recently reported theoretically [15]. Moreover, it is well suited to telecommunication tasks as VCSELs are today wide spread in local and metropolitan networks. It also requires less energy as the threshold current of VCSELs is lower than the

#362410 https://doi.org/10.1364/OE.27.018579
Journal © 2019 Received 19 Mar 2019; revised 15 May 2019; accepted 5 Jun 2019; published 18 Jun 2019

Optics EXPRESS

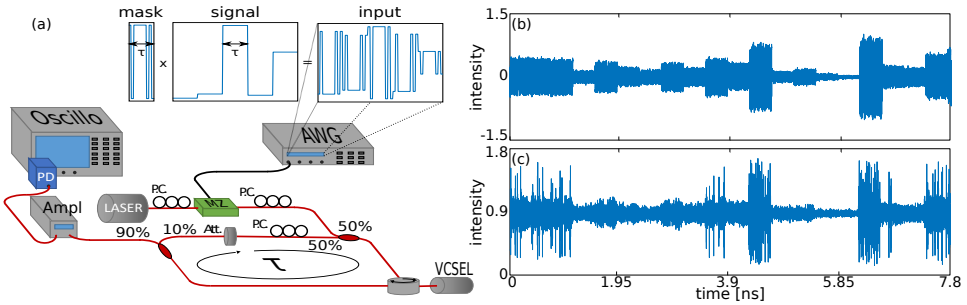

Fig. 1. (a) Scheme of the setup. The signal loaded in the AWG is made by multiplying the input signal by a mask. MZ: Mach-Zehnder madolator, P.C.: polarization Controller, AWG: Arbitrary Waveform Generator, att: attenuator, Oscillo: Oscilloscope, ampl: amplificator, PD: photodiode. (b) masked signal for the input of the reservoir computer. (c) corresponding response of the reservoir.

edge-emitting lasers, and permits higher computation speed thanks to faster VCSEL intern dynamics. Although we suggested recently an extension of the time-delay reservoir architecture using VCSEL polarization dynamics [15], the performance of this architecture has never been verified experimentally.

In this letter, we experimentally prove that reservoir computing indeed benefits from using the polarization dynamics of a VCSEL. This system has already been studied through simulations in our previous work [15]. To exhibit this result, we first consider the dynamics of the experimental system to find the best operating point. We then test our reservoir computer with two different benchmark tasks: chaotic time-series prediction and nonlinear channel equalization. We prove while testing the consistency of the result statistically that operating the reservoir with polarization rotated feedback improves the computing performance.

We consider the set-up shown in Fig. 1(a). The reservoir itself is composed of a VCSEL emitting at 1550 nm from Raycan and an optical feedback loop. Along the feedback loop, the light is going through an attenuator Keysight 81577A (att) which controls the feedback strength and a polarization controller (P.C.) which adjusts the polarization of the feedback and allows switching between two different configurations: isotropic or rotated feedback. The optical delay line is 39 ns-long, as fixed by the length of fiber brought by the packaging of each components in the optical feedback. This imposes the processing speed to be at 25.6 MHz. According to [15], the time separation θ between two nodes for this system has to be around 20 ps to provide the best performance. However due to the frequency limitation imposed by our oscilloscope and our modulator, we have chosen to set this value to $\theta = 100\ ps$. This corresponds to the highest frequency we can record with our oscilloscope, i.e. a Tektronix DPO 71604C 16 GHz bandwidth, and the fastest modulation speed of our Mach-Zehnder modulator. That leads to $N = 390$ virtual neurons spread along the delay-line.

The input of data is made optically through optical injection. The input layer comprises a continuous tunable laser Yanista Tunics T100S. Its polarization is adjusted in order to be aligned with the modulation axis of the modulator. Finally a last polarization controller (P.C.) allows controlling the polarization of the injection. All the input signals are numerically generated: the mask composed of 390 different values (as much as the number of nodes) is randomly generated, taking values in {-1; 1}, then this mask is modulated by the different input values. These signals are loaded in an Arbitrary Waveform Generator (AWG) Tektronix AWG 700002A and generated at 10 GSamples/s and sent to the RF port of the the modulator.

The output layer is composed of an EDFA-amplifier (ampl) and a photodiode (PD) Newport 1544-B 12 GHz bandwidth. The signal of the photodiode is recorded by the oscilloscope at

Optics EXPRESS

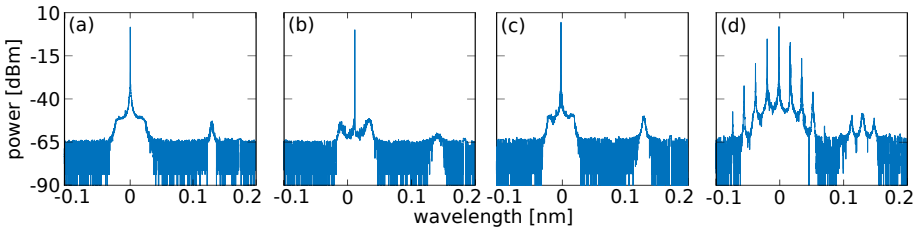

Fig. 2. Experimental optical spectra in different conditions. (a) free running VCSEL, (b) System with feedback and injection (50 μW injection, 18 dB attenuation), (c) VCSEL with parallel feedback, 10 dB attenuation, (d) VCSEL with rotated feedback, 10 dB attenuation.

50 GSamples/s. Using an optical amplifier is mandatory as the power recorded from the VCSEL is lower than the detection threshold of our photodiode. The fiber splitter between the feedback loop and the output layer yields 90% of the total power for the detection. The recorded signals are post-processed using a computer.

We first focus on the dynamical properties of this system. Figure 2 depicts different optical spectra. Figure 2(a) shows the one of the free running VCSEL. All figures are centered on the wavelength of the free-running emission of the VCSEL, which is 1552.88 nm. The bias current is set to 1.5 times the threshold current $I_{th} = 3\ mA$, which corresponds to 4.5 mA. The total output power of the VCSEL is then 166 μW. This current value is chosen as it is the one allowing the best discrimination of the different inputs in the response of the reservoir computer. This has been observed in simulations and it is therefore consistent with our experimental observations. The operating temperature is set to 21°C. In this condition, the VCSEL emits in two linear polarization modes. The power ratio between the two polarization modes is 54.23 dB and their frequency difference is measured to be 16.4 GHz. Note that the suppression ratio is high, but similar to what we simulated in [15], and we still expect an impact of the polarization on the performance. The tuning of the polarization of the feedback loop is made with the lowest attenuation possible (10 dB). This allows exhibiting different dynamics depending on the polarization of the feedback as shown on Figs. 2(c) and 2(d). In these conditions, the VCSEL with rotated feedback exhibits several optical frequencies in both polarization modes (Fig. 2(d)), compared to isotropic feedback, in which the VCSEL shows a cleaner optical spectrum (Fig. 2(c)). Therefore the polarization rotated optical feedback yields a richer polarization nonlinear dynamics when compared to the isotropic optical feedback. While applying injection, the VCSEL exhibits a much narrower peak in its dominant polarization mode (Fig. 2(b)). Indeed the VCSEL is locked at the operating point [16]. The detuning between the master laser and the slave laser is 0.01 nm (-1.05 GHz). The emitted power of the depressed mode is also reduced.

For the operating point, the system is set at the edge of instabilities as it is the best state for a system to perform reservoir computing [17]. This specific point has also been confirmed for our system numerically in [15]. We increase the attenuation and the optical injection power until the system reaches the steady state. This state is reached while applying an attenuation of 18 dB in the optical feedback for both isotropic and rotated feedback configuration, and a mean optical injected power of 50 μW. Figure 2(b) shows the optical spectrum of the setup in such conditions.

In the following the reservoir is kept at this operating point. Figure 1 shows the input and output signals from the reservoir. Figure 1(b) displays a part of the signal used to feed the reservoir computer: nineteen masked input values. Each input value is maintained during $\tau = 39\ ns$. Figure 1(c) shows the response of the reservoir computer corresponding to the input values of Fig. 1(b). The mask allows keeping the reservoir in a transient state during the operation.

Following the procedure previously explained, we have first tested our reservoir with the Sante-Fe series prediction task [18]. This task aims at predicting the next time-step value of

Optics EXPRESS

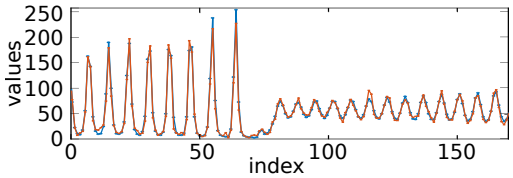

Fig. 3. Example of Santa Fe series prediction: the original Santa-Fe series (blue line and circles), and the predicted series (red line and crosses).

the Santa-Fe chaotic series, from the knowledge of the previous values. We asses the level of performance with the normalized mean square error (NMSE) defined as:

$$NMSE = \frac{1}{N}\frac{\sum_{i=1}^{N}(y(i)-\tilde{y}(i))^2}{\sigma_y}, \tag{1}$$

where N is the number of samples, $y(i)$ is the target signal, $\tilde{y}(i)$ is the estimated signal by the reservoir, and σ_y is the variance of the original signal.

This task has been chosen as it is a well-known task to test reservoir computers, and allows comparing the efficiency of our architecture to other experimental reservoir computer based on semiconductor lasers [14]. In our case, we used the total power of the optical signal as the state for each node, that means the sum of the power in the dominant and depressed polarization modes. 6000 samples are used to train our system, performed with a linear regression. The 2992 other samples are used for testing. In these conditions, we successfully reach a NMSE of 1.9×10^{-2} with parallel feedback. Performance is slightly better with rotated feedback, with a NMSE of 1.6×10^{-2}. Both are the mean results over 3 different training and testing. This is also an order of magnitude lower than the results obtained with other laser-based time delay reservoir computer, even with shorter training and testing sets used in ref. [14]. An example of prediction is given in Fig. 3: the predicted signal is really close to the target signal even for the lowest values, thus leading to a low relative error. As this task is a reconstruction of a chaotic series, the target value is almost continuous. Hence, this task is highly sensitive to the signal-to-noise ratio (SNR). Considering this fact, we suggest that the performance we reached is related to the SNR we can achieve experimentally and which is estimated at about 12 dB.

Since this reservoir computer is first thought to solve telecommunication problems, we have studied the channel equalization task more in depth [19]. This task aims at reconstructing a signal that has been distorted through a nonlinear communication channel. This original signal $d(i)$ is built by drawing symbols randomly in {-3; -1; 1; 3}. The different inputs are first linearly combined as follows:

$$\begin{aligned} q(i) &= 0.08d(i+2) - 0.12d(i+1) + d(i) + 0.18d(i-1) - 0.1d(i-2) + 0.091d(i-3) \\ &\quad -0.05d(i-4) + 0.04d(i-5) + 0.03d(i-6) + 0.01d(i-7). \end{aligned} \tag{2}$$

This signal is then modified using a nonlinear function:

$$u(i) = q(i) + 0.026q(i)^2 - 0.011q(i)^3, \tag{3}$$

The output values $u(i)$ of the nonlinear channel are finally used to feed the reservoir computer, and infer the original inputs $d(i)$. The performance on this task is measured through the symbol error rate (SER). This is the total number of errors committed while performing the task divided by the total number of symbols in the signal. Figure 4(a) presents an example of experimental signal reconstruction in the case of rotated feedback configuration. Only one symbol has been incorrectly reconstructed in the 83^{th} position. In that case, SER is 1.1×10^{-2}

Optics EXPRESS

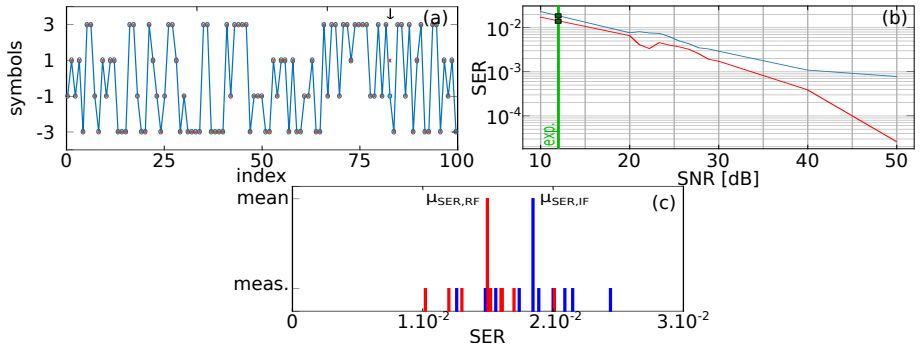

Fig. 4. Results for channel equalization task. (a) experimental prediction for the channel equalization task: the target signal (blue lines and circles) and the predicted signal (red crosses) in case of polarization rotated feedback. arrow points out the error (b) Theoretical SER for different SNR added in the readout layer, for parallel feedback (blue) and perpendicular feedback (red). The green line is set at the experimental level of SNR, green squares show the experimental performance. (c) Experimental results: The shortest strips shows the different SER obtained over different measurement series, the biggest strips shows the mean value, for the parallel feedback (blue) and the perpendicular feedback (red).

As already mentioned, the SNR in the output layer of our system is low, around 12 dB. We therefore run new simulation based on the simulation framework used in [15] to have an insight of the role of this level of noise in the reservoir computer on its performance. These results are shown in Fig. 4(b). It shows the expected performance on nonlinear channel equalization task depending on the SNR of the readout layer, for the two different types of feedback under study. Simulating the reservoir computer with 12 dB of SNR in the output layer yields the SER that is achievable about 1.9×10^{-2} with parallel feedback and 1.5×10^{-2} with perpendicular feedback.

We then run the experimental measurement series for both isotropic and rotated feedback configuration. Figure 4(c) depicts the SER we obtained over the nine measurements we made for each configuration, and the mean SER. Each time, the training was made with 10000 samples, and the testing with 5400 samples, as previously using the total optical power as the state of one node. The mean SER is lower with perpendicular feedback (1.5×10^{-2}) as the one with parallel feedback (2×10^{-2}). Added to that, these results are almost identical to the one theoretically obtained. Considering the low SNR we are able to reach, these results have been statistically analyzed with a one-sided t-test with a significance level of $\alpha = 2.5\%$ to compare the averaged SER obtained from series of SER measurement realized in the isotropic ($\mu_{SER,IF}$) and polarization-rotated feedback ($\mu_{SER,RF}$) configuration, respectively. The null hypothesis $H_0 : \mu_{SER,IF} = \mu_{SER,RF}$ is tested against the alternative hypothesis $H_1 : \mu_{SER,RF} < \mu_{SER,IF}$. We first confirm the normality of the data using a Kolmogorov-Smirnov test [20] and then apply the t-test. We find that the statistics of interest computed from the data (and following a Student's distribution with 15 degrees of freedom) belongs to the rejection region of the test : $(-\infty, -2.131]$. As a result, we reject H_0 in favor of H_1 with significance level $\alpha = 2.5\%$. This implies that we have strong statistical evidence in this low-SNR situation that the polarization rotated feedback allows smaller SER in the nonlinear channel equalization task. This strengthens the first insight we had from the chaotic time series prediction. The experiment conclusively shows the improved performance of the reservoir computer using polarization competition as theoretically predicted in [15].

Figure 4(b) also tells us the way to increase the performance further, i.e. by increasing the SNR. The low SNR is due to the noise added by the amplifier at the readout layer. This amplification is mandatory to detect the low power signal emitted by the VCSEL. A higher SNR can be achieved by either replacing the amplifier with a less noisy one or by increasing the laser output power.

Optics EXPRESS

To conclude, we presented in this article an experimental realization of a time-delay reservoir based on a VCSEL. The laser is used in injection locking mode to perform calculation. Using this particular dynamics, we were able to solve different tasks successfully : the chaos prediction task with a NMSE of 1.6×10^{-2} and nonlinear channel equalization with a SER of 1.5×10^{-2}, both error rates being below the state-of-the-art and at high bit rates. Moreover, we proved experimentally earlier theoretical predictions with large statistical significance : using rotated feedback instead of isotropic allows enhancing the computing performance of a physical reservoir.

Funding

Chaire Photonique: Ministère de l'Enseignement Supérieur, de la Recherche et de l'Innovation; Région Grand-Est; Département Moselle; European Regional Development Fund (ERDF); Metz Métropole; Airbus GDI Simulation; CentraleSupélec; Fondation CentraleSupélec.

References

1. L. K. Grover, "Quantum computers can search arbitrarily large databases by a single query," Phys. Rev. Lett. **79**, 4709–4712 (1997).
2. J. P. Crutchfield, W. L. Ditto, and S. Sinha, "Introduction to focus issue: Intrinsic and designed computation: Information processing in dynamical systems-beyond the digital hegemony," Chaos **20**, 037101 (2010).
3. H. Jaeger and H. Haas, "Harnessing nonlinearity: Predicting chaotic systems and saving energy in wireless communication," Science **304**, 78–80 (2004).
4. K. Vandoorne, P. Mechet, T. Van Vaerenbergh, M. Fiers, G. Morthier, D. Verstraeten, B. Schrauwen, J. Dambre, and P. Bienstman, "Experimental demonstration of reservoir computing on a silicon photonics chip," Nat. Commun. **5**, 3541 (2014).
5. L. Larger, A. Baylón-Fuentes, R. Martinenghi, V. S. Udaltsov, Y. K. Chembo, and M. Jacquot, "High-speed photonic reservoir computing using a time-delay-based architecture: Million words per second classification," Phys. Rev. X **7**, 011015 (2017).
6. J. Bueno, S. Maktoobi, L. Froehly, I. Fischer, M. Jacquot, L. Larger, and D. Brunner, "Reinforcement learning in a large-scale photonic recurrent neural network," Optica **5**, 756–760 (2018).
7. L. Appeltant, M. C. Soriano, G. Van der Sande, J. Danckaert, S. Massar, J. Dambre, B. Schrauwen, C. R. Mirasso, and I. Fischer, "Information processing using a single dynamical node as complex system," Nat. Commun. **2**, 468 (2011).
8. L. Larger, M. C. Soriano, D. Brunner, L. Appeltant, J. M. Gutierrez, L. Pesquera, C. R. Mirasso, and I. Fischer, "Photonic information processing beyond turing: an optoelectronic implementation of reservoir computing," Opt. Express **20**, 3241–3249 (2012).
9. Y. Paquot, F. Duport, A. Smerieri, J. Dambre, B. Schrauwen, M. Haelterman, and S. Massar, "Optoelectronic reservoir computing," Sci. Rep. **2**, 287 (2012).
10. F. Duport, B. Schneider, A. Smerieri, M. Haelterman, and S. Massar, "All-optical reservoir computing," Opt. Express **20**, 22783–22795 (2012).
11. D. Brunner, M. C. Soriano, C. R. Mirasso, and I. Fischer, "Parallel photonic information processing at gigabyte per second data rates using transient states," Nat. Commun. **4**, 1364 (2013).
12. R. M. Nguimdo, G. Verschaffelt, J. Danckaert, and G. V. der Sande, "Simultaneous computation of two independent tasks using reservoir computing based on a single photonic nonlinear node with optical feedback," IEEE Trans. Neural Netw. Learn. Syst. **26**, 3301–3307 (2015).
13. K. Takano, C. Sugano, M. Inubushi, K. Yoshimura, S. Sunada, K. Kanno, and A. Uchida, "Compact reservoir computing with a photonic integrated circuit," Opt. Express **26**, 29424–29439 (2018).
14. K. Hicke, M. A. Escalona-Morán, D. Brunner, M. C. Soriano, I. Fischer, and C. R. Mirasso, "Information processing using transient dynamics of semiconductor lasers subject to delayed feedback," IEEE J. Sel. Top. Quantum Electron. **19**, 1501610 (2013).
15. J. Vatin, D. Rontani, and M. Sciamanna, "Enhanced performance of a reservoir computer using polarization dynamics in VCSELs," Opt. Lett. **43**, 4497–4500 (2018).
16. K. Panajotov, I. Gatare, A. Valle, H. Thienpont, and M. Sciamanna, "Polarization- and transverse-mode dynamics in optically injected and gain-switched vertical-cavity surface-emitting lasers," IEEE J. Quantum Electron. **45**, 1473–1481 (2009).
17. N. Bertschinger and T. Natschläger, "Real-time computation at the edge of chaos in recurrent neural networks," Neural Comput. **16**, 1413–1436 (2004).
18. C. Chatfield and A. S. Weigend, "The future of time series," in *Time series prediction: Forecasting the future and understanding the past,* C. Chatfield and A. S. Weigend, eds. (Addison-Wesley, 1993).
19. V. J. Mathews and J. Lee, "Adaptive algorithms for bilinear filtering," Proc.SPIE 2296, 317-327 (1994).
20. N. L. Johnson, S. Kotz, and N. Balakrishnan, *Continuous Univariate Distributions* (Wiley-Interscience, 1995). Ed. 2, Vol. 2.